$La_{15}Ge_9Z$. Interstitial Derivatives with an Ordered Superstructure of the Mn_5Si_3 Structure Type. Property Trends in a Series of Homologous Intermetallic Phases

Arnold M. Guloy[†] and John D. Corbett*

Department of Chemistry and Ames Laboratory—DOE,[1] Iowa State University, Ames, Iowa 50011-3020

Received November 29, 1995[⊗]

The phases $La_{15}Ge_9Z$, Z = Mn, Fe, Co, Ni, Cu, Ru, C, O, P, have been obtained from reactions of either the elements or suitable binary compounds in sealed Ta containers at 1200−1350 °C. All exhibit an ordered $\sqrt{3}a \times \sqrt{3}a \times c$ superstructure of the Mn_5Si_3 type (La_5Ge_3, La_5Ge_3Z, $P6_3/mcm$) in which two-thirds of the slightly distorted confacial chains of trigonal antiprisms ($La_{6/2}Ge_{6/2}$) have Z bound in alternate, contracted interstitial sites. The room-temperature structures for Z = Mn, Fe, Co, Ni, C, P were refined from single-crystal data (space group $P6_3mc$, Z = 2; for the protypical Fe, a = 15.4810(2) Å and c = 6.8768(3) Å). The unit cell lengths and volumes and d(Z−Z) values show notably smaller variations with Z than in La_5Ge_3Z or related systems. The buffering effect of empty cavities in the commensurate chains and the weak La−La bonding appear to be responsible. Magnetic susceptibility data and XPS core shifts are reported for the Fe and, in part, the Co and Ni phases $La_{15}Ge_9Z$. All three are metallic with decreasing moments of ∼1.83, ∼0.3, and ∼0 μ_B, respectively. In contrast, the Fe-richer La_5Ge_3Fe is a very soft ferromagnet at room temperature. Members of the sequence Fe, La_5Ge_3Fe, $La_{15}Ge_9Fe$ exhibit regularly decreasing moments as well. The Fe $2p_{3/2}$ core levels show a 1.7 eV decrease over the same series, i.e., increasing reduction, while an evidently regular oxidation of La from the element through La_5Ge_3 and $La_{15}Ge_9Fe$ to La_5Ge_3Fe is indicated by a regular overall increase of 2.7 eV in La $3d_{5/2}$ binding energies.

Introduction

Phases with a Mn_5Si_3-type structure have proven to be exceedingly attractive for the exploration of chemical and electronic variables within relatively straightforward intermetallic systems. About 170 binary compounds have been reported to exhibit this structure, principally between the early metals in groups 2−6 (T) and main-group elements (M) of the Al, Si, and As families.[2] At least in the more polar examples, it is relatively easy to assess the number of excess conduction-band electrons beyond those necessary to fill the valence levels of the isolated Si-type atoms. The broad and general interstitial chemistry is found for these phases (originally termed Novotny phases[3]) on filling the $T_{6/2}M_{6/2}$ chains within these, that is, the centers of the confacial trigonal antiprisms ("octahedra") of the T metals on which M atoms bridge all edges of the shared faces. (T atoms in a separate linear chain in the structure do not appear to participate in the chemistry.) We have earlier explored this new chemistry for a range of hosts and found that a wide variety of third elements Z may often be bound quantitatively in the centers of the antiprisms to produce stoichiometric T_5M_3Z phases, stuffed versions of the same structure type. These have been characterized for the substrates Zr_5Sb_3,[4,5] Zr_5Sn_3,[6] Zr_5Pb_3,[7] Ae_5Pn_3 (Ae = Ca, Sr, Ba, Sm, Yb; Pn = As, Sb, Bi),[8,9] La_5Ga_3,[10] and, most particularly, for La_5Ge_3[11] and La_5Pb_3,[12] in which about 18 Z may be bound in each binary host. The Z versatility also allows one to systematically vary properties. For example, it becomes possible to "tune" the three extra conduction electrons in La_5Ge_3 ($5 \times 3 - 3 \times 4 = 3$) to zero with Z = P, As, etc. and thereby to produce valence (Zintl) compounds. The same feature pertains to Ae_5Pn_3Cl etc.[8] On the other hand, incorporation of interstitials such as Si, Ge, or Ga that require more than the three extra electrons into La_5Ge_3 always generates other structure types in which the holes that would otherwise appear in the valence band of La_5Ge_3Z disappear with the formation of main-group (Ge_2 etc.) dimers.[13] These simple chemical interpretations are not so evident, however, when a less electronegative Z like Fe is encapsulated because the added states now lie in or near the ideal valence-conduction band gap or overlap region.

Many of these T_5M_3Z phases turn out to be substantially line phases. However, the synthetic explorations of La_5Ge_3Z chemistry to establish this point and to understand some literature reports regarding supposed "La_5Ge_3" (actually La_5Ge_3O[11]) led us to the serendipitous discovery of a new class of more dilute interstitial compounds, $La_5Ge_3Z_{1/3}$ (=$La_{15}Ge_9Z$) for Z = Mn, Fe, Co, Ni, Cu, Ru, C, O, P. These exhibit a novel ordering of one-third as much Z in a $\sqrt{3} \times \sqrt{3} \times 1$ superstructure of the usual hexagonal La_5Ge_3Z (stuffed Mn_5Si_3 type). The existence of evidently the same superstructure has been noted before for substoichiometric $R_5Si_3C_x$ samples (R = Y, Gd, Ho, Er),[14−17] but no compositional or structural details were established.

[†] Present address: Department of Chemistry, University of Houston, Houston, Texas 77204-5641.

[⊗] Abstract published in *Advance ACS Abstracts,* July 15, 1996.

(1) This research was supported by the Office of the Basic Energy Sciences, Materials Sciences Division, U.S. Department of Energy. Ames Laboratory is operated for DOE by Iowa State University under Contract No. W-7405-Eng-82.

(2) Villars, P.; Calvert, L. D. *Pearson's Handbook of Crystallographic Data for Intermetallic Phases,* 2nd ed.; American Society for Metals: Metals Park, OH, 1991.
(3) Novotny, H.; Benesovsky, F. In *Phase Stability in Metals and Alloys;* Rudman, P. S., Stringer, J., Jaffee, R. I., Eds.; McGraw-Hill: New York, 1966; pp 319−336.
(4) Garcia, E.; Corbett, J. D. *Inorg. Chem.* **1988**, *27*, 2353.
(5) Garcia, E.; Corbett, J. D. *Inorg. Chem.* **1990**, *29*, 3274.
(6) Kwon, Y.-U.; Corbett, J. D. *Chem. Mater.* **1992**, *4*, 1348.
(7) Kwon, Y.-U.; Corbett, J. D. *J. Alloys Comp.* **1993**, *190*, 219.
(8) Hurng, W.-M.; Corbett, J. D. *Chem. Mater.* **1989**, *1*, 311.
(9) Leon-Escamilla, E. A.; Corbett, J. D. *J. Alloys Comp.* **1994**, *206*, L15.
(10) Zhao, J.-T.; Corbett, J. D. *J. Alloys Comp.* **1994**, *210*, 1.
(11) Guloy, A. M.; Corbett, J. D. *Inorg. Chem.* **1993**, *32*, 3532.
(12) Guloy, A. M.; Corbett, J. D. *J. Solid State Chem.* **1994**, *109*, 352.
(13) Guloy, A. M.; Corbett, J. D. Unpublished research.

S0020-1669(95)01515-1 CCC: $12.00

Table 1. Synthesis Conditions and Lattice Dimensions of La_5Ge_9Z Phases

compn	synthesis conditions[a]	lattice parameters Å[b]		V, Å^3	c/a
		a	c		
$La_{15}Ge_9Mn$	S	15.4964(3)	6.884(1)	1431.6(3)	0.4442
$La_{15}Ge_9Fe$	C	15.4810(2)	6.8768(3)	1427.1(1)	0.4442
$La_{15}Ge_9Co$	S	15.4950(2)	6.8686(4)	1428.2(1)	0.4433
$La_{15}Ge_9Ni$	S	15.5001(2)	6.873(1)	1430.0(1)	0.4434
$La_{15}Ge_9Cu$	S	15.5164(3)	6.9005(5)	1438.7(1)	0.4447
$La_{15}Ge_9Ru$	S	15.5180(3)	6.9014(5)	1439.3(1)	0.4447
$La_{15}Ge_9C$	S	15.4674(6)	6.8795(5)	1425.4(2)	0.4448
$La_{15}Ge_9O$	S	15.535(1)	6.758(1)	1412.4(2)	0.4350
$La_{15}Ge_9P$	C	15.4946(3)	6.8649(5)	1435.7(2)	0.4430
$La_{15}Ge_9$(ideal)[c]		15.486(2)	6.878(1)	1428.5(4)	0.4441

[a] S: Binaries and elements sintered at 1250−1350 °C for 10−15 days. C: Prereacted binaries and elements slowly heated to 1200 °C and annealed at 1000 °C for 10 days. [b] Hexagonal, $P6_3mc$ (No. 186), $Z = 2$. Guinier data at $t = 22$ °C, $\lambda = 1.540\,562$ Å. [c] a(superstructure) $= \sqrt{3}a(La_5Ge_3)$.[11]

Experimental Section

Syntheses. The materials used, the synthetic methods, and the general Guinier powder and single-crystal X-ray methods employed have been described before.[5,11] Sintering of pressed pellets either of the elements or of La_5Ge_3 plus elemental Z while sealed within Ta for 10−15 days at 1250−1350 °C in a high-temperature vacuum furnace was again useful and more often gave good single crystals. Reactions within pressed pellets of La, Ge, and an appropriate binary like Mn_3Ge_2, $FeGe_2$, $CoGe_2$, NiGe, $LaCu_2$, La_2O_3, or LaP briefly at 1200 °C and then at 1000 °C for 7−10 days gave good control of stoichiometry and also some single crystals. Arc melting followed by annealing is possible for most products, but this route gives distinctly poorer control of compositions and phase distributions.[5] Synthesis conditions and lattice parameters for all nine examples of the new structure are given in Table 1; the latter were refined by least-squares means from indexed Guinier powder diffraction data with Si as an internal standard. A given $La_{15}Ge_9Z$ phase is readily distinguishable from the analogous La_5Ge_3Z member for all but the oxide by the smaller (sub)cell dimensions of the former which are closer to those of the empty La_5Ge_3.

Negative synthetic results were obtained for Z = Ti, V, Cr, Zn, Cd, B, As, Sb, S, Cl, all of which except Ti and V do form La_5Ge_3Z phases (substoichiometric for both B and C[11]). N and Se were not explored. The phases are less reactive with air than is La_5Ge_3, but chunks still turn into black powders in 2−3 h at room temperature, and they slowly evolve gas from water. The oxide derivative in particular is apparently stable in air for weeks at room temperature. All have a metallic luster.

Semiquantitative SEM/EDX analyses of several members were made on a JEOL JSM-840 instrument. Well-faced crystals mounted in epoxy and polished with sandpaper and leather could be utilized as long as the transfer to the instrument was not delayed. These resulted in atom percent values for Z of 5.6(3) (Mn), 4.4(3) (Fe), 5.9(4) (Co), 3.1(3) (Ni), 3.8(3) (Cu) versus 4.0% ideally. La was found to lie in a range of 58.7(2) (Co) to 60.6(2) (Fe) atom % relative to the ideal 60.0%. The Ge contents calculated by difference ranged from 34.6(3) (Mn) to 36.7(3) (Ni) atom % versus 36.0% expected.

Structural Studies. During the course of this investigation, single-crystal X-ray diffraction data for six $La_{15}Ge_9Z$ members, Z = Mn, Fe, Co, Ni, C, P, were collected at room temperature and refined, the Fe and Co compounds with data from a CAD4 diffractometer and the remainder with data from a Rigaku AFC6R instrument. The 2θ limits of 60, 70, and 65° were employed for Ni, C, and P, respectively, with 55° for the remainder (Mo Kα). In all cases, a hexagonal cell that corresponded to a $\sqrt{3} \times \sqrt{3} \times 1$ expansion of that of La_5Ge_3 (Mn_5Si_3 type, $P6_3/mcm$) type was readily found through standard indexing procedures with the aid of 25 tuned reflections.

The Fe phase was studied first. A 6/*mmm* symmetry was consistent with the axial photograph, and this was also confirmed both by axial (Polaroid) measurements on the diffractometer and by precession (zero and higher level) film studies. A 4-fold redundant data set and three ψ scans were measured. Reflection conditions for data from both the diffractometer and films indicated possible space groups $P6_3/mmc$, $P\bar{6}2c$, and $P6_3mc$, and the last, acentric member proved to be correct. All La and Ge positions were provided by direct methods (SHELXS-86[18]), and the interstitial Fe disposition was revealed by a difference Fourier map. The ψ-scan results did not provide adequate absorption corrections ($\mu = 437$ cm^{-1}) at the stage of a converged isotropic refinement (R, $R_w = 5.5$, 7.3%), and so the numerical DIFABS procedure was applied at the isotropic level, as recommended.[19] This gave final values of $R(F)$, $R_w = 2.6$, 3.4% with well-behaved displacement parameters and reasonable standard deviations. An occupancy refinement for Fe gave a 92.7(1)% value, but this atom lies at the highest symmetry point, and systematic errors, not a real fractional occurrence, were considered likely considering the sizable effect that interstitials have on cavity size. The largest residuals, 1.13 and −1.12 e/Å^3, occurred at (0, 0, 0.625) in the channel near La4 and at (0.41, 0.21, 0.29), respectively. Refinement of the inverted structure showed that the correct enantiomer had been selected first.

The other five structures were refined following confirmation of the Laue symmetry on the diffractometer or indexing of the powder pattern based on the Fe model, and these started with the La and Ge positions in the first structure. Some summary data are listed in Table 2. More information on the diffraction studies and results as well as some anisotropic atom displacement data are given in the Supporting Information. These as well as some F_o/F_c listings are also available from J.D.C.

Other Properties. Magnetic susceptibility data on the Fe, Co, Ni examples over 6−300 K were secured with the aid of a Quantum Design MPMS-SQUID facility. Better signals, important for weakly magnetic or diamagnetic samples, were obtained with the aid of an improved container that held the sample in place. This was made by sliding and fitting an 8.5-cm-long, 3-mm-o.d. silica rod in one end of a 21-cm-long, 3-mm-i.d. fused silica tube. The rod was fixed in the tube by fusing their common ends. The sample pieces were weighed (~20 mg) and placed in the open end of the silica container within a helium atmosphere glovebox. Another 3-mm silica rod, ~12 cm long, was fitted into the open end of the silica container such that the sample was pressed between the two rods. The open end of the outer piece was next inserted into a short, narrow rubber tube to make a temporary airtight fit. The container was taken out of the glovebox and carefully sealed under He at a point 8.5 cm above the sample (to minimize distortion). An identical standard container filled only with He was made to provide the diamagnetic correction for the sample holder.

XPS data for the Fe and Ni phases were secured with the aid of an AEI-200B spectrometer and Al Kα radiation. Samples were mounted on In within an attached glovebox, and the binding energies were referenced to adventitious carbon at 285.0 eV. Argon ion etching was sometimes done to clean the sample surface. This resulted in larger signals for Z, but no significant shift of the core peaks of the constituent atoms.

Results and Discussion

The formation of nine isostructural members of a new $La_{15}Ge_9Z$ family has been established, namely, for Z = Mn, Fe, Co, Ni, Cu, Ru, C, O, P (Table 1). The crystal structures have been refined for six of these, Z = Mn, Fe, Co, Ni, C, P. The positional and isotropic-equivalent displacement parameters for the atoms in the parent $La_{15}Ge_9Fe$ are listed in Table 3, while corresponding data for the five other closely related examples (in the same setting) are contained in the Supporting Information. Interatomic distances within all six are listed in Table 4 for later comparisons.

(14) Al-Shahery, G. Y. M.; Jones, D. W.; McColm, I. J.; Steadman, R. *J. Less-Common Met.* **1982**, *85*, 233.
(15) Al-Shahery, G. Y. M.; Jones, D. W.; McColm, I. J.; Steadman, R. *J. Less-Common Met.* **1982**, *87*, 99.
(16) Al-Shahery, G. Y. M.; McColm, I. J. *J. Less-Common Met.* **1983**, *92*, 329.
(17) Button, T. W.; McColm, I. J. *J. Less-Common Met.* **1984**, *97*, 237.
(18) Sheldrick, G. M. SHELXS-86. Universität Göttingen, Germany, 1986.
(19) Walker, N.; Stuart, D. *Acta Crystallogr.* **1983**, *A19*, 158.

Table 2. Data Collection and Refinement Parameters for $La_{15}Ge_9Z$ Structural Determinations[a]

	Z					
	Mn	Fe	Co	Ni	C	P
fw	2792.0	2792.9	2796.0	2795.8	2749.1	2768.0
d, g cm^{-3}	6.48	6.50	6.50	6.49	6.40	6.40
2θ(max), deg	55	55	55	60	70	65
no. of indep refl, var	814, 50	688, 50	688, 49	1235, 49	933, 48	736, 49
abs coeff (Mo Kα), cm^{-1}	327.8	436.9	439.4	299.8	312.3	313.4
R,[b] %	2.8	2.6	1.8	2.5	2.4	2.6
R_w,[c] %	2.8	3.4	3.2	2.2	3.2	3.4

[a] Lattice dimensions in Table 1. The space group is $P6_3mc$ (No. 186), $Z = 2$. [b] $R = \sum||F_o| - |F_c||/\sum|F_o|$. [c] $R_w = [\sum w(|F_o| - |F_c|)^2/\sum w(F_o)^2]^{1/2}$; $w = \sigma_F^{-2}$.

Table 3. Positional and Isotropic-Equivalent Thermal Parameters for Prototypical $La_{15}Ge_9Fe$ ($P6_3mc$)

	x	y	z	B_{eq},[a] Å^2
La1(12*d*)	0.01768(5)	0.34207(5)	0[b]	0.78(1)
La2(6*c*)	0.41368(4)	2*x*	0.7401(1)	0.71(2)
La3(6*c*)	0.25333(4)	2*x*	0.2771(1)	0.70(2)
La4(6*c*)	0.08020(4)	2*x*	0.7245(1)	0.71(1)
Ge1(6*c*)	0.13280(8)	2*x*	0.2721(2)	0.78(4)
Ge2(6*c*)	0.46610(9)	2*x*	0.2613(2)	0.84(4)
Ge3(6*c*)	0.19995(8)	2*x*	0.7115(2)	0.64(4)
Fe(2*b*)	$^1/_3$	$^2/_3$	0.5160(3)	1.89(4)

[a] $B_{eq} = (8\pi^2/3)\sum_i\sum_j U_{ij}a_i^*a_j^*\vec{a}_i\vec{a}_j$. [b] Fixed parameter.

The Structures. Figure 1 shows $La_{15}Ge_9Fe$ in a [001] projection of the contents of two unit cells along *c* plus parts of the surrounding cells. The structure contains two distinct types of chains or columns of confacial trigonal antiprisms of La (open ellipsoids), one along 0, 0, *z* (La4) and a pair along $^1/_3$, $^2/_3$, *z* and $^2/_3$, $^1/_3$, *z* (La2, La3). All edges of the shared $La_{6/2}$ faces in these chains are bridged by Ge (solid ellipsoids; Ge1 on the first chain type, Ge2 around the second, and Ge3 between the two types). The elevations and packing are such that each edge-bridging Ge is also exo to a La vertex in an adjoining chain that has nearly the same *z* coordinate. Finally, the tunnels along *c* between the foregoing chains contain slightly zigzag chains of interbonded La1 atoms.

The basic arrangement is a 3-fold supercell in the *a*−*b* plane of La_5Ge_3 (Mn_5Si_3 type) as well as of the stuffed La_5Ge_3Z examples.[11] Four adjoining columns or chains define the hexagonal subcell of the latter (dashed lines), the long diagonal axis of which ($\sqrt{3}a$) is now the axial length of the supercell. Ordering of Z differentiates the two chain types; the centers of alternate trigonal antiprisms in the chains along $^1/_3$, $^2/_3$, *z* and $^2/_3$, $^1/_3$, *z* are occupied while those in the other along 0, 0, *z* are entirely empty. Portions of the half-filled and empty columns (with different orientations) are shown in Figure 2. It should be noted that the Ge atoms about these two chains in this illustration are in part the same atoms, since all exhibit complementary edge-bridging and interchain exo bonding roles. The empty chains are bridged to six half-filled members while the half-filled chains have three of each kind as neighbors. The average antiprism heights are necessarily all the same, but binding of interstitials into alternate polyhedra in two-thirds of the chains gives a Peierls-like distortion and alternating long (empty) and compressed (filled) antiprisms in these. The La2−La3 distances between adjoining faces thus alternate between ∼3.83 and ∼4.27 Å. Figure 3 shows a portion of two adjoining half-filled chains and the alternation in elevation that is reflected in the *c*-glide about $(1\bar{1}0)$.

The bifunctional edge-bridging and exo Ge atoms are coplanar with the shared La faces in La_5Ge_3 and in the isopointal, stuffed La_5Ge_3Z, but these deviate modestly from planarity here because of the distortions produced by fractional interstitial filling. The largest displacements of this type, both in bridges between different column types and mainly in the edge-bridging functions, are 0.38 Å for Ge1 relative to the $(La4)_3$ plane in the empty chain and 0.20 Å for Ge3 about $(La2)_3$ in the half-filled example. Distortions of the half-filled chains, Figure 2, also appear to be the reason for the change in the La1 chain angles along this string from 180° in the parent to 164.2(±0.2)° in the superstructure examples. The Ge environment about these La1 atoms remains a twisted trigonal antiprism (Figure 1). This chain again remains the least affected by the interstitial chemistry. Distances from La1 to the surrounding Ge atoms are generally 0.02−0.07 Å greater than distances found to those atoms about the antiprismatic columns but still 0.05 Å less on average than in La_5Ge_3. The La−Ge distances fall into two fairly clear groups, ∼3.12 Å for edge-bridging and ∼3.23 Å for exo functions, very similar to those in La_5Ge_3.

Structural Variations with Z. Trends in lattice constants alone scarcely illuminate the nature of the distance and, presumably, bonding changes that occur throughout this series of compounds, which were our principal reason for the many structural refinements (in addition to confirmation of the stoichiometries). Only La_5Ge_3 and La_5Ge_3Cr have been quantified structurally before, while just cell dimensions were established for 18 other stuffed La_5Ge_3Z examples.[11] In comparison, the *c* dimensions in the superstructures (Table 1) vary over a ±0.2 Å range, expanding most for Cu and Ru and contracting especially for O (but not for C). These more or less parallel, but are smaller than, similar effects in La_5Ge_3Z except that the value with oxygen there is essentially unchanged. Oxygen actually produces the largest *a* for all $La_{15}Ge_9Z$ and, relative to $\sqrt{3}a$, in La_5Ge_3O as well, evidence of the substantial constriction and distinctive reapportioning of the lattice during oxygen encapsulation. Carbon shows a smaller constriction but an opposite change in *c*/*a*. The relative increases in *c* and *V* with the 3d metals are far less here than in La_5Ge_3Z, presumably because of the buffering effects of the antiprismatic cavities. The changes in interatomic distances within the entire $La_{15}Ge_9Z$ family, Table 4, are particularly remarkable because of the universally small changes. The largest differences are ∼0.06 Å in the edges of the shared La2−La2 and La3−La3 triangles in the half-filled chains, with Fe generally giving the largest effect and Mn, the smallest followed by Co. All La−La contacts are less than in La_5Ge_3. The bridging and exo La−Ge distances all expand relative to La_5Ge_3, but only in a range of ∼0.02 and ∼0.03 Å, respectively, and without much discrimination among Fe, Co, Ni and even from C for that matter. These two trends are, by the way, consistent with earlier band calculations in that electrons removed on oxidation of the La_5Ge_3 substrate with Z generally come from bands that are La−La bonding but La−Ge antibonding.[11]

The most distinct surprises are in the La−Z separations which (a) range only between 2.702(3) and 2.669(2) Å and (b) order as Fe > Mn, P, Ni > C ≃ Co. This trend is certainly not evident in the cell dimensions or volumes because of other distance

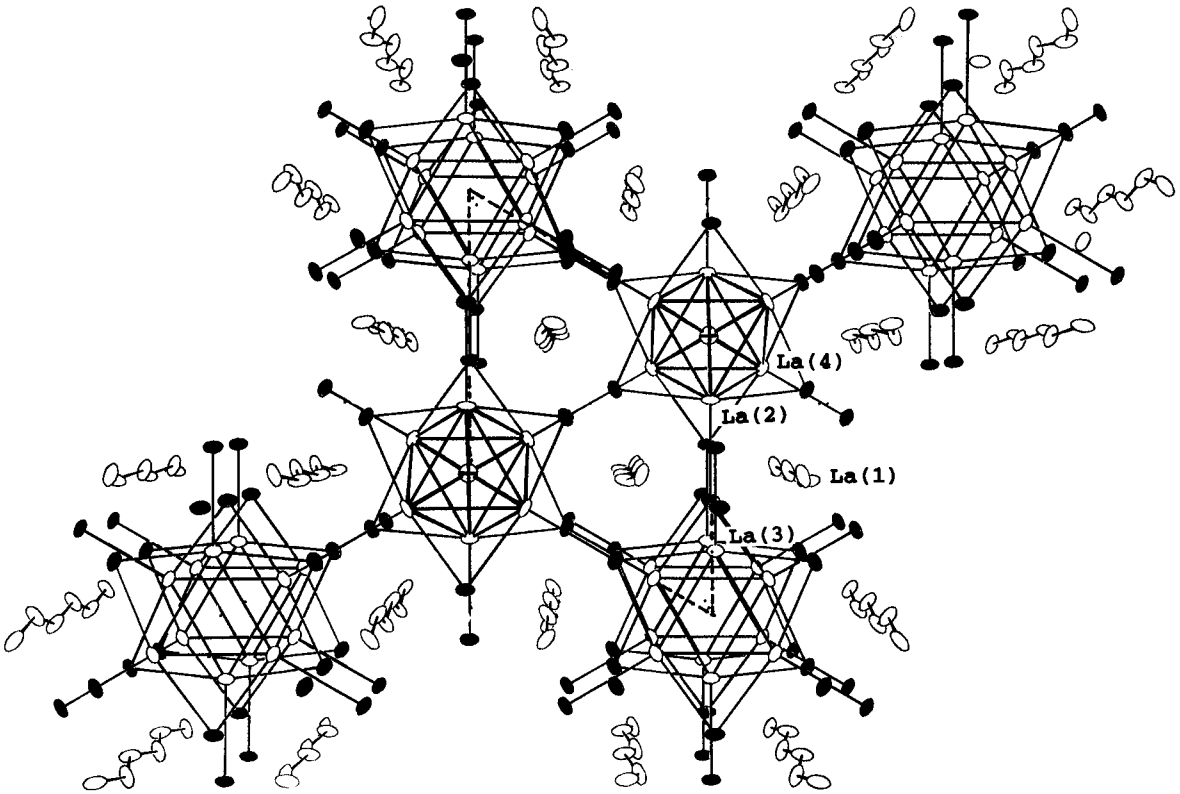

Figure 1. [001] projection of a two-cell depth for $La_{15}Ge_9Fe$. Cavities in the two $^1_\infty[La_{6/2}Ge_{6/2}]$ chains within the cell are alternately occupied by Fe, while those along 0, 0, *z* are empty. The dashed lines mark the Mn_5Si_3-type subcell of La_5Ge_3 etc. Open ellipsoids represent La, solid Ge, and crossed Fe (90% probability).

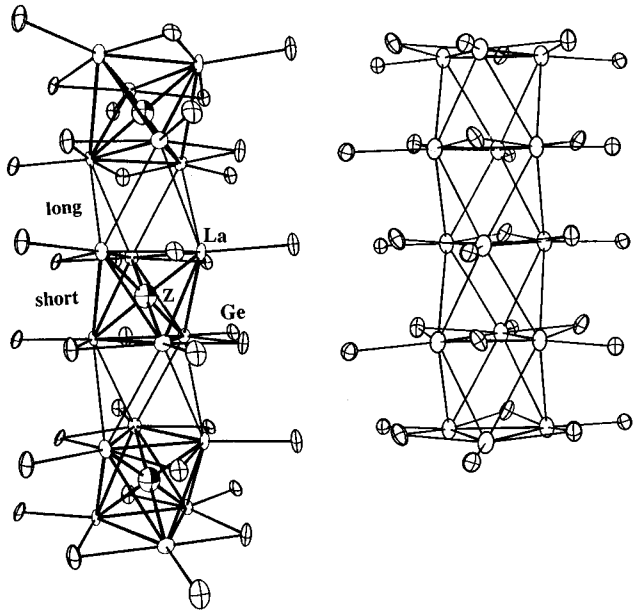

Figure 2. Side views of the two $^1_\infty[La_{6/2}Ge_{6/2}]$ chain types in $La_{15}Ge_9Fe$: left, chain half-filled by Fe (note the Peierls-like distortion); right, an empty chain. Note that the exo Ge atoms shown on both chain types are edge-bridging on others. (La are open, Ge crossed, and Fe shaded 90% ellipsoids.)

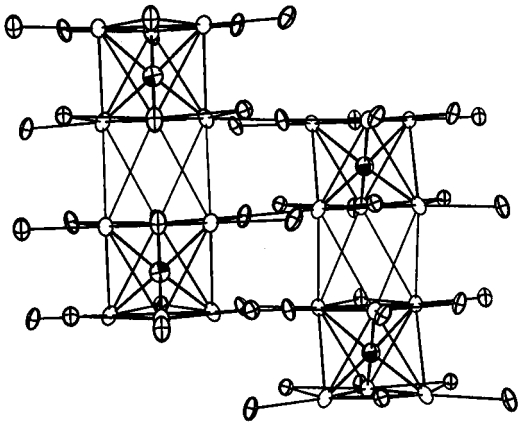

Figure 3. Orientation of two neighboring half-filled columns in the center of the $La_{15}Ge_9Fe$ cell, Figure 1. (La are open, Fe shaded, and Ge crossed ellipsoids.)

contributions (La−La, La−Ge) thereto, and the reasons for the listed variations are not very clear chemically either. The general contraction of the cavity on Z binding is emphasized in Figure 4 as $\bar{d}$(La−Z) for what might be the most interpretable series, Mn−Ni relative to the empty host. However, the values for C and P are in fact scarcely different, 2.67 and 2.69 Å, respectively. The effect can also be seen in an inverse way in the relative distortions within the La2−La3 columns, which are plotted in Figure 5 as the differences between the long and short *d*(La2−La3) in the Mn−Ni series. (The former distances, not listed in Table 4, fall in a narrow range around 4.27 Å.) The same differences for C and P are also very similar to that for Ni, 0.443 and 0.446 Å, respectively. The relatively small radius of Co (Figure 4), but not of C, is also reflected in this distortion. The minimum radius and maximum contraction for cobalt is unexpected and uncorrelated with usual scales of radii (below).

A speculative possibility may derive from the fact that the valence electron count per centered unit in $La_{15}Ge_9Co$ ($15 \times 3 - 9 \times 4 + 9 = 18$) is just that found to be electronically optimal in many isolated octahedral halide clusters of rare-earth metals or zirconium centered by transition metals, in the octahedral $Pr_6(Co)I_{12}^{3-}$, for instance.[20] Thus, the neighboring Mn, Fe, etc.

(20) Hughbanks, T.; Corbett, J. D. *Inorg. Chem.* **1988**, *27*, 2022.

Table 4. Selected Distances (Å) in La_5Ge_3Z Phases[a]

		Z					
		Mn	Fe	Co	Ni	C	P
La1−La1	x2	3.4707(5)	3.4709(2)	3.4709(2)	3.4693(3)	3.4719(1)	3.4638(1)
La1−La2		3.800(1)	3.760(2)	3.774(1)	3.775(1)	3.763(1)	3.766(1)
La1−La2		4.001(1)	4.009(1)	4.009(1)	3.994(1)	3.990(1)	4.009(1)
La1−Ge1		3.180(2)	3.192(2)	3.202(2)	3.187(1)	3.188(2)	3.192(2)
La1−Ge1		3.297(2)	3.291(2)	3.281(2)	3.293(1)	3.287(2)	3.280(2)
La1−Ge2		3.198(2)	3.217(2)	3.226(2)	3.210(1)	3.216(2)	3.212(2)
La1−Ge2		3.274(2)	3.267(2)	3.257(2)	3.268(1)	3.265(2)	3.261(2)
La1−Ge3		3.202(1)	3.190(2)	3.171(2)	3.196(1)	3.188(2)	3.178(2)
La1−Ge3		3.289(2)	3.301(2)	3.306(1)	3.306(1)	3.300(2)	3.314(2)
La2−La2	x2	3.6714(1)	3.7315(2)	3.695(1)	3.7206(1)	3.7233(9)	3.702(1)
La2−La3	x2	3.828(1)	3.843(1)	3.808(1)	3.830(1)	3.835(1)	3.822(1)
La2−Ge2[a]		3.246(1)	3.227(1)	3.245(1)	3.226(1)	3.225(1)	3.230(2)
La2−Ge3	x2	3.130(1)	3.125(1)	3.1408(5)	3.119(1)	3.124(1)	3.116(2)
La2−Z		2.692(2)	2.701(3)	2.664(2)	2.690(1)	2.670(3)	2.694(3)
La3−La3	x2	3.6524(3)	3.7156(2)	3.682(1)	3.702(1)	3.710(1)	3.694(1)
La3−Ge1[b]		3.255(1)	3.232(1)	3.248(1)	3.230(1)	3.225(1)	3.227(2)
La3−Ge2	x2	3.122(1)	3.1065(5)	3.114(1)	3.120(1)	3.105(1)	3.123(2)
La3−Ge3		3.349(1)	3.312(2)	3.317(1)	3.307(1)	3.303(2)	3.304(2)
La3−Z		2.694(2)	2.702(3)	2.665(2)	2.689(1)	2.668(3)	2.690(3)
La4−La4		3.6536(3)	3.7247(3)	3.670(1)	3.727(1)	3.7104(9)	3.700(1)
La4−Ge1	x2	3.133(1)	3.123(1)	3.128(1)	3.1395(5)	3.1233(8)	3.139(1)
La4−Ge3[b]		3.251(2)	3.212(1)	3.229(1)	3.229(1)	3.214(1)	3.243(2)
La−Z (ave)		2.693(3)	2.702(4)	2.664(3)	2.690(1)	2.669(4)	2.692(4)

[a] d(La−Ge) < 3.40 Å, d(La−La) < 4.01 Å. [b] Exo La−Ge bonds.

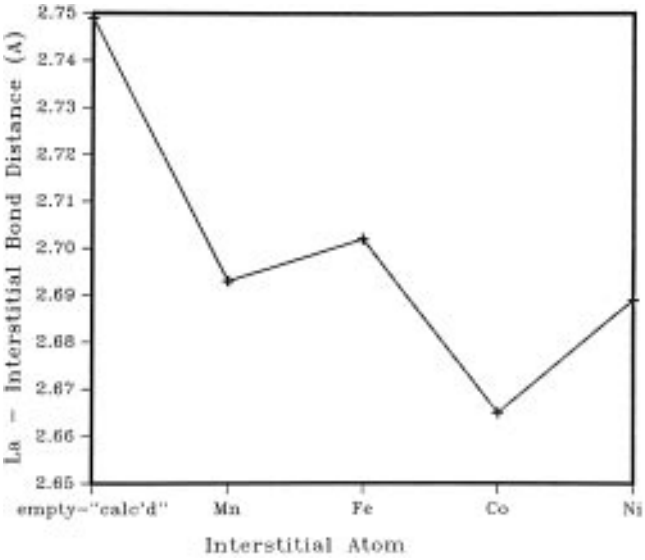

Figure 4. Variation of the La−interstitial (Z) distances in $La_{15}Ge_9Z$ for Z equal to nothing (the centroid in La_5Ge_3), Mn, Fe, Co, and Ni.

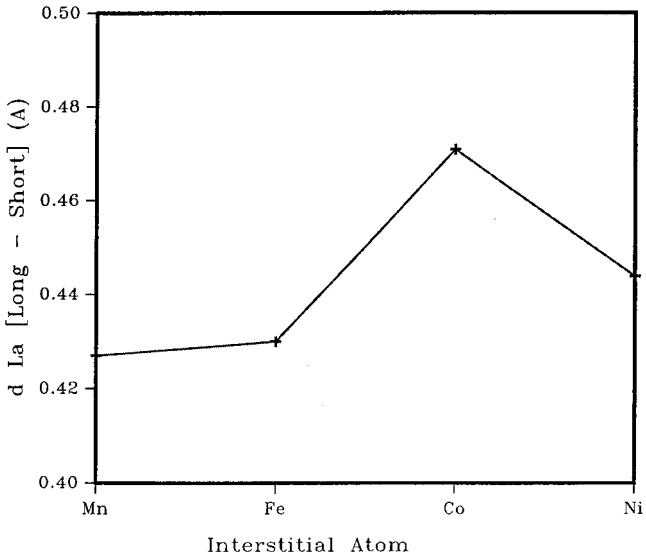

Figure 5. Variation of the difference in La−La separations along the half-filled chain (Figure 2a) in $La_{15}Ge_9Z$ for Z = Mn−Ni.

have fewer or more than 18e and are less well bound. Nonetheless, this simple assessment seems a bit problematical; the suggested localization is not altogether consistent with evidence that these compounds are presumably metallic and, in part, paramagnetic (below). Further studies are necessary.

The small differentiation among interstitial radii in the $La_{15}Ge_9Z$ series is also in distinct contrast to analogous measures in interstitial-stabilized cluster systems, for example, the distantly comparable, isolated $Zr_6(Z)X_{12}$-type halide clusters (Z = Be−N, Al−P, Cr−Ni, Ge) in a wide variety of structures, where relative changes in d(Zr−Z) parallel customary metallic or covalent radii.[21] For example, the observed distances in $Li_xZr_6Cl_{15}Z$ phases increase slowly (by 0.047 Å) between Mn and Ni.[22] Nonetheless, these correspond to a $\bar{d}$(La−Z) value of ∼2.68 Å for the 3d metal interstitials when converted by means of the difference in crystal radii for La vs Zr (0.31 Å, CN 6[23]), a value close to those observed here. (Use of the metallic single-bond differences instead gives a 2.61 Å prediction.) The average La−Fe distances in $La_{12}I_{17}Fe_2$, a complex network of separate $La_6(Fe)I_{12}$-type clusters, is 2.81 Å, 0.11 Å greater than here, perhaps because of matrix restrictions afforded by the large iodine atoms.[24] In contrast, the interstitial radii of Fe and C differ by 0.12 Å in isostructural $M_xZr_6Cl_{18}Z$ compounds,[25] not the 0.03 Å found here, and the La−C distance prediction (corrected from Zr−C as above) would be 2.52 Å, 0.15 Å less than observed in $La_{15}Ge_9C$. Comparisons of the measured 2.67 Å with other La−C distances can only be somewhat indirect. One parallel in the limited number of comparable T_5M_3Z phases that have been characterized dimensionally occurs for the electron-richer Zr_5Sn_3C.[6] The Zr−C distance found for this, 2.459 (1) Å, and the 2.35 Å in ZrC

(21) Corbett, J. D. *J. Alloys Compd.* **1995**, *229*, 10.
(22) Zhang, J.; Corbett, J. D. *Inorg. Chem.* **1991**, *30*, 431.
(23) Shannon, R. D. *Acta Crystallogr.* **1976**, *A32*, 751.
(24) Lulei, M.; Martin, J. D.; Corbett, J. D. *J. Solid State Chem.*, in press.
(25) Zhang, J.; Corbett, J. D. *Inorg. Chem.* **1993**, *32*, 1566.

(NaCl)[26] similarly convert to 2.77 Å and 2.66 Å for La−C (vs 2.67 Å observed), not the contracted 2.52 Å deduced from halide clusters. The choice is rather broad and confusing. Among La−C compounds, the lanthanum acetylides LaC_2 and La_2C_3 are not very useful standards because the anion is clearly anisotropic in contact distances and bonding. The R_2C (inverse $CdCl_2$) structures known for Tb_2C and Dy_2C[27] yield smaller La−C values of 2.58 ± 0.01 Å for La−C when converted with crystal radii. In the same way, the less symmetric, double-metal-layered Y_2Cl_2C, Gd_2XC (X = Cl, Br), and Gd_3Cl_3C with carbon in compressed, antiprismatic surroundings[28] lead to La−C expectations of 2.60−2.64 Å. The average for the four halide examples, 2.616 Å, is 0.05 Å less than observed here.

The largest problem appears to be in the unusually large cluster around the interstitial carbon atom in $La_{15}Ge_9C$, the only structure with a second-period Z that was quantified, while a smaller novelty is associated with a 0.03−0.05 Å reduction in *d*(La−Co) relative to those for its neighbors. Judging from our studies of many other T_5M_3Z systems, these clusters do not collapse as much as they should for small Z, probably because of restrictions provided by the neighboring commensurate array of empty cavities and chains in this structure. Perhaps La−La repulsive interactions in the somewhat polar $La_{15}Ge_9Z$ structures are another factor that limits the cavity contraction, particularly since the La−La bonding conduction band contains only a few electrons, nominally only 0.33 electron per La in the carbide [(15 × 3 − 9 × 4 − 4)/15].

Presumably numerous $R_{15}Tt_9Z$ members with the $La_{15}Ge_9Fe$ structure exist for other R and Tt (Si, Ge, Sn, Pb) elements. We have earlier noted the formation of $La_{15}Sn_9C$ and $La_{15}Sn_9O$ according to powder diffraction data.[29] The formation of a $\sqrt{3} \times \sqrt{3}$ superstructure of the Mn_5Si_3 type has been observed in $R_5Si_3C_x$ systems, R = Y, Gd, Ho, Er, but no further information was provided.[14−17] The difficulty in identifying this superstructure with only powder data originates with the weakness of the few extra lines. Intensities of the most distinctive of these [(101), (311), (321), (531)] are calculated to be only 1.4−4.4% of I_{max} for $La_{15}Ge_9O$ and 2.8−5.9% for the present iron compound. However, some supercell reflections were always found among the 25 orientation reflections randomly located and tuned during each of our single-crystal diffractometer studies. A somewhat related $\sqrt{3} \times \sqrt{3}$ structure has also been seen for $Mn_5Ge_{2.7}Ga_{0.3}$ in space group $P6_3/mmc$.[30] Here the atoms remain on planes at $z = 0$, $^1/_4$, etc., suggesting that interstitial sites are not fractionally occupied in an ordered way. The superstructure may be induced by the fractional substitution of Ga on Ge2 sites (in our numbering scheme) along with ∼13% vacancies on the equivalent of the La2 positions.

Other Properties. Magnetic susceptibility data for powdered $La_{15}Ge_9Z$, Z = Fe, Co, Ni, were collected to clarify their relationship with La_5Ge_3Fe (below). All are expected to be metallic so a Pauli paramagnetic term presumably adds to any Curie−Weiss behavior. This is evidently seen in the 1/*M* vs *T* results for $La_{15}Ge_9Fe$ shown in Figure 6, from which an upper limit for the magnetic moment, 1.83 μ_B, is estimated. The paramagnetic property decreases thereafter; the cobalt compound

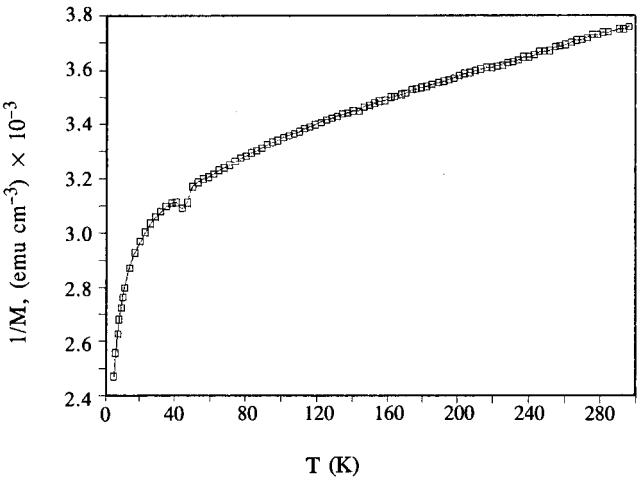

Figure 6. Inverse volume magnetization of $La_{15}Ge_9Fe$ vs *T* at 0.5 T. (The blip presumably reflects an external O_2 impurity.)

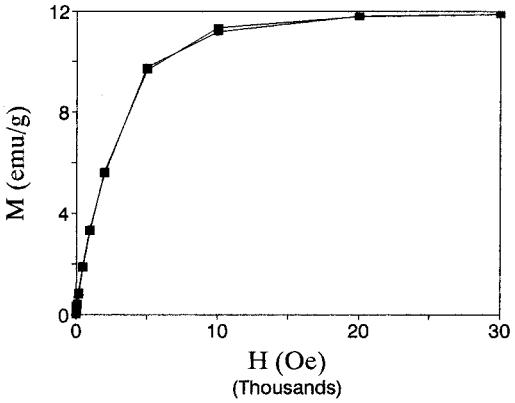

Figure 7. Magnetic (*M*) hysteresis cycle for La_5Ge_3Fe as a function of field (kOe) at 100 K. Note the absence of a reverse field for quenching.

gives ∼0.3 μ_B over 6−60 K (0.1 T) with $\chi_0 \sim 1.8 \times 10^{-3}$ emu mol^{-1}, while any moment for the nickel phase is basically indistinguishable from the temperature dependence of its Pauli paramagnetism over 6−295 K. These moments compare with 2.2, 1.72, and 0.6 μ_B for the respective metals Fe, Co, Ni.[31]

A useful comparison is with La_5Ge_3Fe and its analogues, for which we report some new data. Although the iron compound decomposes on slow cooling (to $La_{15}Ge_9Fe$ and an evidently substituted La_4Ge_3), single-phase samples can be quenched from ∼1400 °C.[11] The fully stuffed La_5Ge_3Fe shows a vanishing temperature dependence of the magnetization between 5 and 400 K, 3.1×10^{-3} emu g^{-1} at 1000 Oe. It appears to be a very soft ferromagnet, as judged by both the field dependence of *M* at 50 and 300 K (Supporting Information) and the hysteresis measurements plotted in Figure 7. The saturation magnetic moment, 1.93 μ_B per Fe, is comparable to that of the metal (2.2 μ_B), and the value of μ_{eff} corresponds to two unpaired electrons per center. Intrachain coupling of the Fe atoms in La_5Ge_3Fe via conduction electrons and Fe 4s states seems likely since these centers are $c/2 = 3.54$ Å apart. The fact that the La_5Ge_3Fe sample remains ferromagnetic at room temperature of course requires adequate coupling between chains, too. In view of the large distance between pairs of germanium-bridged chains (8.96 Å), coupling via the intervening pair of La1 chains seems more plausible (see the subcell in Figure 1), and the calculated La2−La1 overlap population in La_5Ge_3Fe is fairly

(26) Krikorian, N. H.; Wallace, T. C.; Anderson, J. L. *J. Electrochem. Soc.* **1963**, *110*, 587.
(27) Atoji, M. *J. Chem. Phys.* **1981**, *75*, 1434.
(28) Simon, A.; Mattausch, Hj.; Miller, G. J.; Bauhofer, W.; Kremer, R. K. In *Handbook on the Physics and Chemistry of Rare Earths*; Gschneidner, K. A., Eyring, L., Eds.; North-Holland; Amsterdam, 1991; Vol. 15, p 222.
(29) Kwon, Y.-U.; Rzeznik, M. A.; Guloy, A.; Corbett, J. D. *Chem. Mater.* **1990**, *2*, 546.
(30) Noga, A. S.; Sichevich, O. M.; Zavodnik, V. E.; Fundamenskii, V. S.; Griń, Yu. N. *Sov. Phys. Crystallogr.* **1991**, *36*, 490.
(31) Cullity, B. D. *Introduction to Magnetic Materials*; Addison Wesley: Reading, MA, 1972; p 129.

Table 5. Core Binding Energies (eV) in La_5Ge_3, La_5Ge_3Fe, $La_{15}Ge_9Z$, and the Elements by XPS

	phase					
level	La_5Ge_3	$La_{15}Ge_9Fe$	La_5Ge_3Fe	$La_{15}Ge_9Ni$	element[a]	Fe_2O_3[a]
La $3d_{5/2}$	837.2	838.2	838.5	836.2	835.8	
$3d_{3/2}$	854.0	853.8	854.2	852.9	852.6	
Ge 3d	26.2	26.0	26.2	26.6	29.4	
Fe $2p_{3/2}$		705.3	705.8		707.0	710.9
$2p_{1/2}$		718.9	719.0		720.1	724.5

[a] Moulder, J. F.; Stickle, W. F.; Sobel, P. E.; Bomben, K. D. *Handbook of X-Ray Photoelectron Spectroscopy*; Perkin-Elmer Corp.: Eden Prairie, MN, 1992.

sizable, 0.104.[11] Iron atoms in the chains in the $La_{15}Ge_9Fe$ superstructure are about twice as far apart (6.88 Å), and the coupling is correspondingly much weaker.

Q-method measurements[32] on La_5Ge_3Fe indicate that it is metallic with a resistivity of ~80 $\mu\Omega$ cm at room temperature with a temperature dependence of $+0.53\%\ K^{-1}$. The host La_5Ge_3 has a comparable resistivity, a $+0.95\%\ K^{-1}$ resistivity coefficient, and a Pauli-like paramagnetism ($\sim 5.5 \times 10^{-6}$ emu mol^{-1}) over 100−300 K. The neighboring elements in La_5Ge_3Co and La_5Ge_3Ni show only a Pauli-like paramagnetism, $\sim 5 \times 10^{-4}$ emu mol^{-1}, that is temperature independent (±~3%) over 50−300 K. Extended Hückel band calculations on La_5Ge_3Fe[11] indicate that the iron's fairly localized and unsplit d states fall around E_f, with the much greater mixing of La 5d with the slightly higher lying Fe 4s presumably being responsible for magnetic exchange coupling along the chains. Interstitial elements to the right of Fe are expected[33,34] to exhibit increasingly narrow and more tightly bound d states in these same hosts, as is observed in both series: ferromagnetic La_5Ge_3Fe, Pauli-paramagnetic La_5Ge_3Co and La_5Ge_3Ni, and, in the more dilute examples, paramagnetic $La_{15}Ge_9Fe$, weakly paramagnetic $La_{15}Ge_9Co$, and substantially Pauli-paramagnetic $La_{15}Ge_9Ni$.

The X-ray photoelectron spectra (XPS) of these phases nicely support the redox and charge transfer concepts that are implicit in our prior descriptions of these compounds. The low-resolution valence spectra were, as usual, not very informative, although apparent Fermi edges were visible for La_5Ge_3, $La_{15}Ge_9Z$, Z = Fe, Ni, and La_5Ge_3Fe, consistent with their evident (poor) metal characteristics. The core shifts for the group listed in Table 5 are more useful. The two types of La atoms were not resolved, as expected, but clear shifts of the $3d_{5/2}$ binding energies to higher values relative to La metal (by 1.5−2.7 eV) were observed, evidence of oxidation with the addition of first Ge and then two different proportions of Fe. According to the numbers, the Ge 3d binding correspondingly decreases from the element by ~3 eV, but a marked change in the nature of the Fermi energy reference for Ge on compound formation makes interpretation of this result more complex. The Fe 2p core values in La_5Ge_3Fe and the electron-richer $La_{15}Ge_9Fe$ are lower than in the element by ~1.2 and ~1.7 eV, respectively, as expected, and are in the opposite direction to the effect of oxidation on formation of Fe_2O_3. These results are consistent with the concept that iron is in effect somewhat reduced by the dominant, more electropositive La host. A small amount of charge transfer to Fe was also suggested by charge-consistent extended Hückel calculations.[11] The $La_{15}Ge_9Ni$ XPS data were less useful, as the unlisted Ni 2p results were masked by La $3d_{3/2}$.

It is pleasing to see how much chemistry can be observed within such metallic hosts as La_5Ge_3 and how much the products exhibit what seem to be more-or-less sensible chemical effects. With ~150 known examples of Mn_5Si_3-type binary phases available, the breadth of compounds possible is large indeed. Other intermetallic structure families also afford new interstitial chemistry, the Cr_5B_3, Yb_5Sb_3, and Th_3P_4 types, for example.[12,35,36]

Acknowledgment. The authors thank J. E. Ostenson, D. K. Finnemore, D. C. Johnston, J. W. Anderegg, and L. Daniels for the use of equipment for, or assistance in, measurements of physical and structural properties.

Supporting Information Available: Tables S1−S3, giving data collection and refinement details, positional data for $La_{15}Ge_9Z$ with Z = Mn, Co, Ni, C, P, and anisotropic displacement parameters for the six structures, and Figure S1, showing plots of magnetization vs field for La_5Ge_3Fe at 50 and 300 K (6 pages). Ordering information is given on any current masthead page.

IC9515158

(32) Shinar, J.; Dehner, B.; Beaudry, B. J.; Peterson, D. T. *Phys. Rev.* **1988**, *B37*, 2066.
(33) Varma, C. M.; Wilson, A. J. *Phys. Rev. B* **1980** *22*, 3805.
(34) Andersen, O. K. In *Highlights of Condensed Matter Physics*; Bassani, F., Fumi, F., Tossi, M. P., Eds; North-Holland: New York, 1985.
(35) Leon-Escamilla, E. A.; Corbett, J. D. *J. Alloys Compd.* **1994**, *206*, L15.
(36) Leon-Escamilla, E. A.; Corbett, J. D. Unpublished research.